Available online at www.sciencedirect.com
SCIENCE DIRECT
Fusion Engineering and Design 81 (2006) 327–333
Fusion Engineering and Design
www.elsevier.com/locate/fusengdes

# The cascading pebble divertor for the spherical tokamak power plant

G.M. Voss [a,*], A. Bond [b], S. Davis [a], M. Harte [a], R. Watson [c]

[a] *EURATOM/UKAEA Fusion Association, Culham Science Centre, Abingdon, Oxfordshire, OX12 3DB, United Kingdom*
[b] *Reaction Engines Ltd., Stanford-in-the-Vale, Oxfordshire, United Kingdom*
[c] *Faculty of Chemical Engineering, University of Surrey, Guildford, Surrey, United Kingdom*

Received 1 February 2005; received in revised form 16 August 2005; accepted 16 August 2005
Available online 18 January 2006

**Abstract**

The design of a power plant based on the spherical tokamak (ST) is being developed in order to explore its potential advantages. The plasma is operated in a double null configuration, forming both an upper and lower divertor. In order to accommodate the high erosion rates and heat fluxes developed in the divertors, a system based on a cascading flow of silicon carbide pebbles is being developed. The pebbles flow into the upper divertor where they fall as a toroidal curtain, which intercepts the divertor particle flux. The pebbles then flow under gravity through ducts to the lower divertor where they form a similar curtain. The bulk temperature of the pebbles rises to about 1150 °C although the outer surface is transiently heated to about 1800 °C. The pebbles pass out of the vacuum chamber into holding tanks and then into a fluidised bed heat exchanger. Here the pebbles are cooled down to about 340 °C and dust and damaged pebbles are removed. The pebbles are transferred to an upper tank by a pneumatic conveyor where the remaining gas is removed and the pebbles flow into the upper divertor again.


*Keywords:* Cascading; Pebble; Divertor; Spherical tokamak

## 1. Introduction

The conceptual design of the ST power plant (STPP) has been previously reported [1–3], its main parameters are shown in Table 1 and the load assembly is shown in Fig. 1. The design of the divertor of the STPP is particularly demanding due to the high heat fluxes and high sputtering rates that limit the performance of conventional solid surface divertors. In order to overcome these two issues, it has been proposed to apply the cascading pebble divertor concept [4] to the ST power plant [2]. This paper presents the current status of the design of this cascading pebble divertor system.

* Corresponding author at: EURATOM/UKAEA Fusion Association, Culham Science Centre, Abingdon, Oxfordshire, OX12 3DB, United Kingdom. Tel.: +44 1235 46 6553; fax: +44 1235 46 6256.
*E-mail address:* garry.voss@ukaea.org.uk (G.M. Voss).

0920-3796/$ – see front matter. 
doi:10.1016/j.fusengdes.2005.08.090

Table 1
Power plant parameters

| Parameter | Value |
|---|---|
| Major radius/minor radius (m) | 3.4/2.4 |
| Plasma elongation/triangularity | 3.2/0.55 |
| Plasma current/rod current (MA) | 31/30.2 |
| Normalised beta | 8.2 |
| Confinement rel. to IPB98(y, 1) | 1.4 |
| Safety factor on axis and edge | 3, 13 |
| Electron den. vol. avge/central ($m^{-3}$) | $1.1/1.4 \times 10^{20}$ |
| Temperature:vol. avge, central (kV) | 19.2, 24.0 |
| NBI current drive power (MW) | 60 |
| Total fusion/net electrical power (GW) | 3.1/1.1 |
| Average neutron wall loading ($MW/m^2$) | 3.5 |

## 2. The cascading pebble divertor

The cascading pebble divertor system produces a primary divertor target surface that intercepts the bulk of the divertor particle energy and allows it to be transported out of the machine as heat in the temperature rise of the pebbles. The pebbles are passed through a fluidised bed heat exchanger, which cools them before they are returned for a further pass through the cascade. The pebble flow enters the load assembly at the top divertor where it splits into two flows.

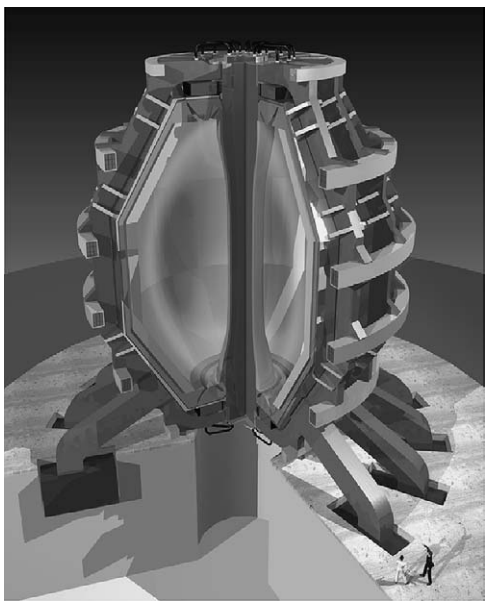

Fig. 1. 3D view of STPP.

One flow forms a curtain of cascading pebbles across the inboard divertor leg. It then flows, under gravity, through ducts in the inboard shield to the lower divertor, where it again forms a cascading flow across the inner divertor leg before flowing out of the load assembly. The other flow forms a cascading curtain across the upper outboard divertor leg then flows through channels in the steel structure between the blanket modules, to the lower outboard divertor leg. Here it forms a cascading curtain of pebbles across the particle flux before also flowing out of the load assembly. These emerging pebble flows have a flow rate of about 450 kg/s and pass into holding tanks. These act as air lock chamber pairs. Once one tank is full, the flow is directed to the other tank of the pair, and the first full tank is isolated from the vacuum chamber, filled with helium gas and its contents flow out into one of two large fluidised bed heat exchangers. These heat exchangers have internal gas cooled, cooling pipes, which extract the bulk of the heat from the pebbles while they are fluidised by a modest flow of helium gas at a pressure of about 10 bar. The high-grade heat removed by the 80 bar helium in the cooling pipes is mixed with the 80 bar helium gas from the blanket modules, which is input to the steam cycle. As the pebbles are cooled, they flow to the top of the fluidised bed where they can flow out of the fluidised bed into one of the pneumatic conveyors, which transport the pebbles back to the top of the machine using dense phase slug flow. The pebbles flow into an annular tank where the helium pressure is only about 1 bar. This gas is then pumped away in a multistage pumping system, to a central helium storage tank. Finally, the pebbles flow under gravity into the top divertor and the cycle repeats. In this way, all helium gas is recycled and the number of mechanical moving parts is kept to a minimum, which offers high reliability. The system is shown schematically in Fig. 2.

## 3. System analysis

### 3.1. Divertor power loads

Under steady state conditions the power arriving at the divertor targets is due to the alpha particle power and the neutral beam injected power. It is assumed here that 50% ($K_{rad}$) of this power can be radiated from the plasma to the first wall by the addition of impurity

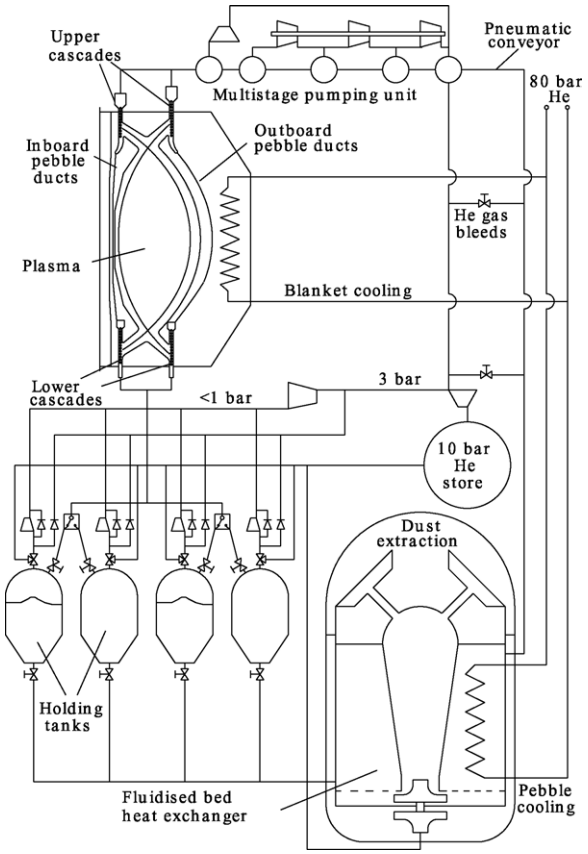


Fig. 2. Cascading pebble divertor schematic.

gases such as argon, as well as Bremstrallung radiation. The ST power plant is operated in a double null configuration and it is assumed that 50% ($K_{\text{D-null}}$) of the power goes to each divertor. When operated in the double null configuration the majority of the divertor power goes to the outboard leg of the ST [3]. Experimental evidence from MAST shows that about 95% ($K_{\text{out}}$) of the power flows to the outboard side (although this varies, depending on the conditions) and a similar split in power is assumed here. The power to each outboard/inboard divertor legs is given by:

$$Q_{\text{out/in}} = (Q_{\alpha} + Q_{\text{NBI}})\, K_{\text{rad}}\, K_{\text{D-null}}\, K_{\text{out/in}} \quad (1)$$

### 3.2. Estimate of SOL thickness

The mid-plane scrape-off-layer (SOL) thickness, $h$, was estimated using a number of theoretical models together with MAST data. These scalings and their $h$ predictions for the collisional SOL cases are described in detail in [3] and the average value for the inner and outer targets are shown in Table 2. The SOL widths at the targets can be broader than those at the mid-plane due to the poloidal flux expansion, $f$, which was estimated from the free-boundary equilibria for the ST power plant [3].

Table 2
Pebble power density parameters

| Parameter | Inner | Outer |
|---|---|---|
| Power to each leg (MW) | 8.5 | 161.5 |
| Radius of the target (m) | 1.6 | 3.15 |
| Avge SOL width $h$ (mm) | 55.2 | 18.9 |
| Poloidal field at target (T) | 0.375 | 0.94 |
| Total field at target (T) | 3.759 | 2.12 |
| Angle $A$ (°) | 5.73 | 26.3 |
| Poloidal flux expansion, $f$ | 1 | 3.5 |
| Max power density (MW/m$^2$) | 25 | 46 |
| $D^+/T^+$ gyro radii (mm) | 0.9/1.1 | 1.6/1.9 |

The power variation across the SOL at the target is an exponential in which $fh$ is the $1/e$ width. A small part of the power diffuses into the private plasma zone side of the separatrix to form a narrower exponential profile as shown in Fig. 3. It is assumed here that this private zone exponential has a $1/e$ width which is 50% that of the main SOL.

### 3.3. Power density on the pebbles

The magnetised plasma in a conventional aspect ratio tokamak normally impinges on the continuous target surface at a shallow toroidal angle, typically 5° due to the ratio of total to poloidal fields. However, in the ST the toroidal field is relatively low giving a higher toroidal angle, typically 25°. The target of the cascading pebble divertor is not continuous and the power density experienced by the pebbles is the parallel power density. The ratio of the poloidal to parallel power density is also dependant on the ratio of these field values and is defined as $\sin A = B_{\text{pol}}/B_{\text{total}}$. Another important factor in considering the power density incident on the pebbles is the gyro radius of the particles in the magnetised plasma. The gyro radii for the main plasma particles are shown in Table 2, assuming an ion temperature, $V$, of 500 eV. These results show the ions have a gyro radius comparable to the radius of pebbles. This ensures the ions approach the pebble surface

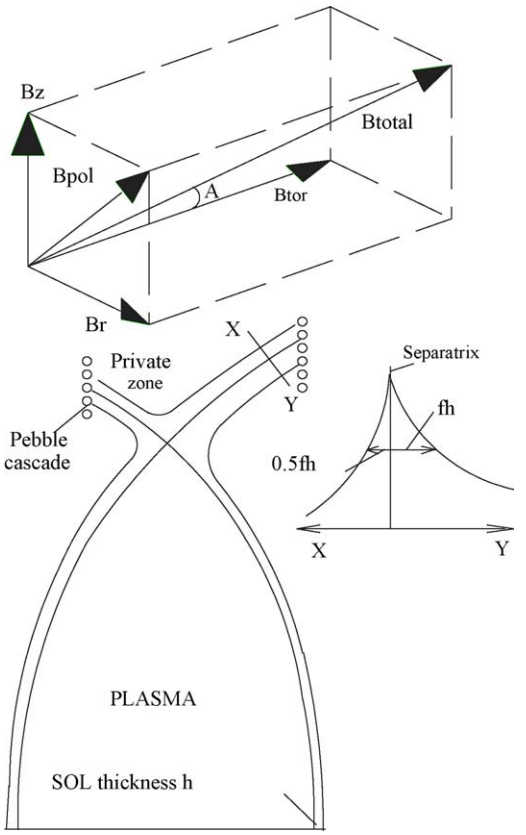


Fig. 3. SOL widths and magnetic fields at target.

from all directions and the flux is applied over the full surface area of the pebble.

This effect is complemented by the fact that the pebbles will be rotating as they fall under gravity through the divertor plasma. Hence, the peak power density seen by an un-shadowed pebble as it passes through the exponential flux profile is given by:

$$\hat{P}_{\text{out/in}} = \frac{Q}{12\pi\, R_{\text{Target}} h\, f \sin A} \tag{2}$$

## 4. Cascade flow rate and transmission

Experimental work carried out by Beverloo et al. [5] on the flow of granular materials through a rectangular orifice show the flow rate $W$ is given by:

$$W = 44.4\rho_{\text{B}} A' \sqrt{g D'_{\text{h}}} \tag{3}$$

$\rho_{\text{B}}$ is the bulk density of the flow, $A'$ and $D_{\text{h}}{}'$ are the effective area and hydraulic diameter given by:

$$D'_{\text{h}} = \frac{4(b-kd)(l-kd)}{2(l+b+2kd)}, \quad A' = (b-kd)(l-kd) \tag{4}$$

where $k$ is a dimensionless constant depending on particle shape and surface properties. The value of $k$ was determined by Beverloo for a variety of materials to be $1.4 \pm 0.1$. $l$ and $b$ are the slot length and width and $d$ is the pebble diameter. In the tests carried out by Beverloo the diameter of the hopper was large compared to the characteristic dimension of the orifice. This leads to a 3-dimensional re-organisation of the pebbles as they flow towards and into the orifice. However, the systems being evaluated here have a delivery chute or hopper whose length is the same as that of the slot, which leads to a 2-dimensional re-organisation of the pebbles as they enter the slot. To account for these differences in the approach flow conditions a linear scale factor $C$ was introduced. The full flow equation in SI units is then:

$$W = \frac{44.4\sqrt{2}}{60} C\rho_{\text{s}} (1-\varepsilon) \sqrt{g} \frac{(l-kd)^{3/2}(b-kd)^{3/2}}{\sqrt{l+b-2kd}} \tag{5}$$

Here $\rho_{\text{S}}$ is the solid material density and $\varepsilon$ is the void fraction which measurements showed to be 0.415.

Two cascade flow rate test rigs were constructed and a series of tests carried out on each using various pebble sizes and materials, slot widths and lengths. The first used an inclined chute to deliver the pebbles to the slot at its end which is representative of that needed for a demonstration of the cascading pebble divertor on the MAST ST. The second test rig had a vertically orientated hopper, which is more representative of the geometry proposed for the ST power plant. Both rigs gave results, which agreed to within 10% of the above expression using a value of the constant $C$ of 1.56.

The opacity of the falling curtain is a function of the pebble diameter, flow rate, curtain thickness and the distance below the slot and can be predicted by starting with Beer's law. A prediction based on this approach was developed and tested by Okui et al. [6] and a modified version of this is used here. The full

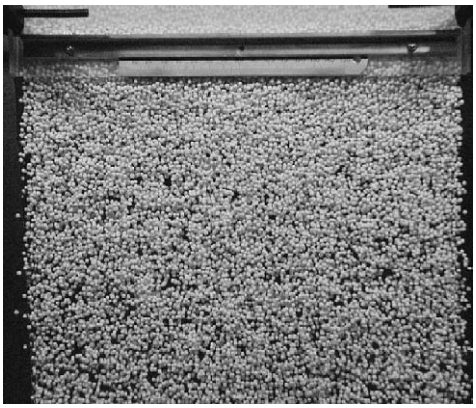

Fig. 4. Front view of pebble cascade.

expression for the opacity of the curtain is:

$$1-\frac{I}{I_0}=1-\exp\left\{-\frac{3W}{2\rho_s(l-kd)d\sqrt{2gh+\left(\frac{W}{\rho_s(1-v)(l-kd)(b-kd)}\right)}}\right\} \quad (6)$$

This expression is derived fully in [7] and was tested by analysing the results of fast photography of the falling curtain. Results showed agreement between measured and calculated opacity to be within 10%. A typical photo of the cascade is shown in Fig. 4. Assuming a drop height to the plasma separatrix of 0.8 m in the outer leg, which has a pebble flow rate of 450 kg/s through a 22 mm wide slot, gives a pebble initial velocity of 0.65 m/s, a final velocity of 4m/s, a pebble heating time of 35ms and a cascade opacity is >90%.

## 5. Pebble thermal and stress analysis

Analytical expressions for the temperature and thermal stress distributions generated within the pebble were first used, with constant material properties, for systems analysis studies. Once the optimised pebble size of 3.2 mm had been determined, finite element thermal and stress analysis was performed with non-linear material properties and the exponential heating rates determined in Section 3 were used. The centre and outer surface temperature profiles for a silicon carbide pebble with a 50-μm outer layer of tungsten are shown in Fig. 5. This shows the temperature of the outer

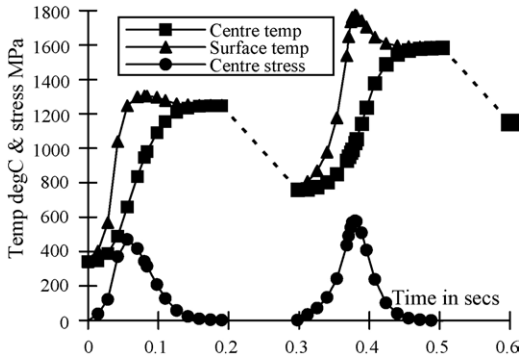


Fig. 5. Transient temperature and stress profiles.

surface rapidly rises as the pebble passes through the exponential flux profiles of the upper outer divertor leg and then equilibrates and radiates heat to its neighbours before it passes through the lower outer divertor leg. This causes the bulk pebble temperature to drop from 1250 to 750 °C. The lower divertor leg again rapidly heats the outer surface of the pebbles to about 1800 °C before the pebbles reach a thermal equilibrium temperature of 1150 °C. The thermally induced tensile stress at the centre of the pebble is also shown in Fig. 5 and peaks at 450 and 600 MPa on the first and second heating cycle. This secondary stress may be relieved as cracks start to form within the silicon carbide. Cyclic tests using lasers to rapidly heat the pebble surface are planned to help determine the materials strength under this loading.

## 6. Sputtering of pebble surfaces

The ions approaching the pebble target have sufficient energy to eject atoms from the surface by physical sputtering. The rate at which the target material is sputtered by this process, $\dot{m}$, is given by:

$$\dot{m} = \frac{m_w \sum Y_i x_i}{N_{AV}} \frac{P_{DIV}}{2q_e V} \quad (7)$$

where $Y_i$, sputtering yield from species $I$; $x_i$, fraction of total ions of species $I$; $P_{DIV}$, power to the divertor pebble targets; $m_w$, atomic mass of target.

An estimate of the sputtering rate due to deuterium, tritium and helium ions is made here assuming:

(1) Half the divertor power is carried by the electrons.

Table 3
Sputtering analysis results

| | Silicon carbide | | Tungsten | |
|---|---|---|---|---|
| Energy (eV) | 500 | 1000 | 500 | 1000 |
| $\sum Y_i x_i$ | 0.065 | 0.074 | 0.005 | 0.009 |
| Tonnes/year | 93.3 | 105.0 | 62.3 | 124.8 |
| $m^3$/year | 30.1 | 33.8 | 3.2 | 6.5 |

(2) The ions are accelerated to twice their approach energy by the electric field generated by the electrons and strike the surfaces at normal incidence.
(3) The contribution from the impurity ions is small.
(4) Plasma composition is 45.8%T, 45.8%D, 8.4%He.

The sputtering yield data given in [8] was used to estimate the sputtering rates, which are shown in Table 3. This shows that for SiC pebbles 105 tonnes per year of SiC will be sputtered, which is about 75% of the total mass of the pebbles assuming a total inventory of 2000 million 3.2 mm diameter pebbles. If the pebbles have a 50 μm thick tungsten coating then this coating would be sputtered at a rate of 125 tonnes per year and is completely removed in about 7 months of continuous operation at an 80% duty cycle. Although the total mass of sputtered material is similar for the two cases the volume of material removed is about 6 times less for tungsten.

## 7. Fluidised bed heat exchanger

The fluidised bed heat exchanger shown in Fig. 6. The hot pebbles, ≈1150 °C, are driven from the holding tanks into the lower end of the main annular chamber where they mix with cool fluidising helium gas. This reduces the pebble temperature to ≈1000 °C before the pebbles pass over the internal array of cooling tubes. These tubes contain helium gas at 80 bar with an inlet temperature of 300 °C and an outlet temperature of 600 °C. This counter-flow arrangement cools the pebbles and the fluidising gas down to about 340 °C by the time they reach the top of this chamber, from where they are transported by six pneumatic conveyors to the top of the power core. Tungsten dust generated by sputtering, may become weakly attached to the pebbles and be carried into the fluidised bed. Here the attrition between the pebbles will remove the dust and it will be carried by the fluidising gas flow to the top of the chamber.

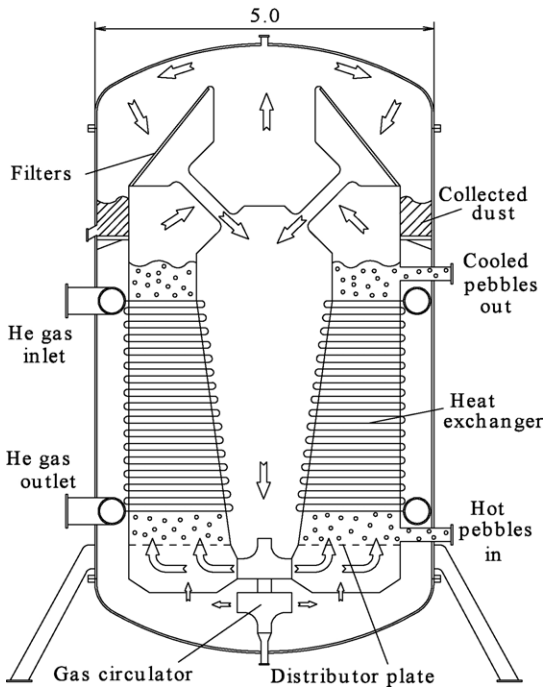


Fig. 6. Fluidised bed heat exchanger.

This dust laden gas flow then passes through inclined mechanical filters, which remove the bulk of the dust, which is collected in an annular chamber at the base of the filters. A gas circulator driven by a helium turbine provides the fluidisation gas flow. This is incorporated into the base of the chamber, which removes the need for rotating seals.

## 8. Pebble manufacturing trials

Manufacturing trials of the pebbles were carried out to demonstrate the process feasibility and estimate the production costs. Two different types of silicon carbide were investigated: pressed and sintered powder (Hexalloy SA) and reaction bonded (REFEL). The REFEL material proved more difficult to manufacture and also has a lower maximum operating temperature than the Hexalloy. The pressed SiC manufacturing process leaves a belt around the equator of each pebble, which must be ground off. The tungsten coating process has been successfully demonstrated based on a chemical vapour deposition process and a micrograph

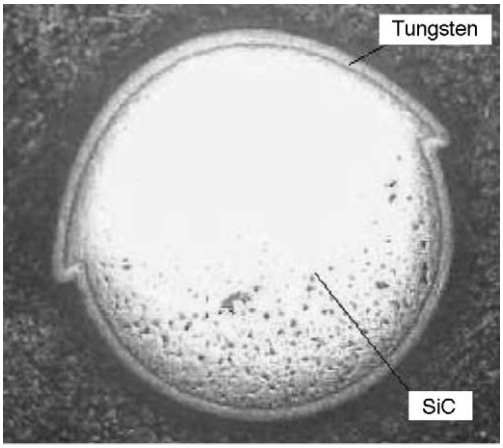


Fig. 7. Section through W coated SiC pebble.

showing the section through a coated Hexalloy pebble is shown in Fig. 7.

## 9. Summary and conclusions

The high heat flux and erosion rates in power plant divertors has led to consideration of a cascading pebble divertor system. This system is particularly suited to the ST due to its relatively low parallel power density and offers the advantages of a solid tungsten surface that is continuously replenished. Systems analysis coupled with experimental work and manufacturing trials have been used to develop the design. Further work is needed to improve the prediction of the divertor power densities and further development of the systems and components is required to demonstrate their performance.

The ST power plant study, together with data from the MAST and NSTX experimental programmes, continues to show that the ST is a strong candidate for future economic power generation.

## Acknowledgements

This work is jointly funded by the UK Engineering and Physical Sciences Research Council and by EURATOM.

## References

[1] G.M. Voss, S. Allfrey, A. Bond, Q. Huang, P.J. Knight, H.R. Wilson, A conceptual design of a spherical tokamak power plant, Fusion Eng. Des. 51–52 (2000) 309–318.
[2] G.M. Voss, A. Bond, J.B. Hicks, H.R. Wilson, Development of a ST power plant, Fusion Eng. Des. 63 (2002) 65–71.
[3] H.R. Wilson, J.-W. Ahn, R.J. Akers, D. Applegate, R.A. Cairns, J.P. Christiansen, Integrated plasma physics modelling of the Culham steady state ST fusion power plant, Nucl. Fusion 44 (2004) 917–929.
[4] K. Matsuhiro, M. Isobe, Y. Ohtsuka, Y. Ueda, M. Nishikawa, Operating windows of the pebble divertor, Nucl. Fusion 41 (2001) 827–832.
[5] W.A. Beverloo, H.A. Leniger, J. Van De Velde, The flow of granular solids through orifices, Chem. Eng. Sci. 15 (1961) 260–269.
[6] T. Okui, Performance characteristics of pebble flow for the pebble divertor, Fusion Eng. Des. 61–62 (2002) 203–208.
[7] S.E. Johnson, R.B. Thorpe, G.M. Voss, Transmissivity of a falling pebble curtain for nuclear fusion reactors, in: Proceedings of the 7th World Congress of Chemical Engineering, 2005.
[8] W. Eckstein, C. Garcia-Rosales, J. Roth, W. Ottenberger, Sputtering Data, Max-Planck Institute for Plasma Physics, IPP 9/82 1993.